Cellular mechanisms of IL-17-induced blood-brain barrier disruption

Jula Huppert,[*,†,1] Dorothea Closhen,[*,1] Andrew Croxford,[†,1] Robin White,[*] Paulina Kulig,[‡] Eweline Pietrowski,[*] Ingo Bechmann,[§] Burkhard Becher,[‡] Heiko J. Luhmann,[*] Ari Waisman,[†,2] and Christoph R. W. Kuhlmann[†,2]

[*]Institute of Physiology and Pathophysiology and [†]First Medical Department, Johannes Gutenberg-University Mainz, Mainz, Germany; [‡]Department of Pathology, Institute of Experimental Immunology, University Hospital of Zürich, Zürich, Switzerland; and [§]Institute of Anatomy, University of Leipzig, Leipzig, Germany

ABSTRACT **Recently T-helper 17 (Th17) cells were demonstrated to disrupt the blood-brain barrier (BBB) by the action of IL-17A. The aim of the present study was to examine the mechanisms that underlie IL-17A-induced BBB breakdown. Barrier integrity was analyzed in the murine brain endothelial cell line bEnd.3 by measuring the electrical resistance values using electrical call impedance sensing technology. Furthermore, in-cell Western blots, fluorescence imaging, and monocyte adhesion and transendothelial migration assays were performed. Experimental autoimmune encephalomyelitis (EAE) was induced in C57BL/6 mice. IL-17A induced NADPH oxidase- or xanthine oxidase-dependent reactive oxygen species (ROS) production. The resulting oxidative stress activated the endothelial contractile machinery, which was accompanied by a downregulation of the tight junction molecule occludin. Blocking either ROS formation or myosin light chain phosphorylation or applying IL-17A-neutralizing antibodies prevented IL-17A-induced BBB disruption. Treatment of mice with EAE using ML-7, an inhibitor of the myosin light chain kinase, resulted in less BBB disruption at the spinal cord and less infiltration of lymphocytes *via* the BBB and subsequently reduced the clinical characteristics of EAE. These observations indicate that IL-17A accounts for a crucial step in the development of EAE by impairing the integrity of the BBB, involving augmented production of ROS.—Huppert, J., Closhen, D., Croxford, A., White, R., Kulig, P., Pietrowski, E., Bechmann, I., Becher, B., Luhmann, H. J., Waisman, A., Kuhlmann, C. R. W. Cellular mechanisms of IL-17-induced blood-brain barrier disruption. *FASEB J.* 24, 1023–1034 (2010). www.fasebj.org**

Key Words: multiple sclerosis · neuroinflammation · reactive oxygen species

Multiple sclerosis (MS) is an autoimmune inflammatory disease of the CNS that is characterized by sclerotic lesions found throughout the brain white matter (1). It is well documented that breakdown of the blood-brain barrier (BBB) is an early and central event in MS pathogenesis (2). Under physiological conditions, the BBB represents a tight barrier between the circulating blood and the CNS and is formed by dense tight junction (TJ) proteins, which seal the space between adjacent brain endothelial cells (BECs). Disruption of the BBB is a crucial event that is involved in the entry of inflammatory cells into the brain, which is a prerequisite for the formation of MS lesions (3).

Previously, it was demonstrated that monocyte transmigration through the BBB is increased after stimulation of BECs with proinflammatory cytokines (4). Specifically, it has been demonstrated that IL-17A-producing T [T helper 17 (Th17)] cells impair BBB integrity by disrupting tight junctions by the mutual action of IL-17A and IL-22 (5). However, little is known about the mechanisms by which IL-17A mediates its effects. IL-17A is a proinflammatory cytokine, first described in 1993 (6). High expression of IL-17A is associated with MS (7) and also with many other autoimmune inflammatory diseases, including rheumatoid arthritis (8), inflammatory bowel disease (9), and systemic lupus erythematosus (10). Treatment with IL-17A-blocking antibodies revealed a beneficial effect on the development and severity of experimental autoimmune encephalitis (EAE), an animal model of MS 11,12). In addition to levels of proinflammatory cytokines, the level of reactive oxygen species (ROS) is increased in MS (13). Oxidative stress is known for its deleterious effects, which can cause enhanced permeability of the BBB (14, 15). Moreover, opening of the BBB and oxidative stress are known to be involved in the pathogenesis of EAE (2, 16). The increased expression of antioxidant enzymes such as superoxide dismutase 1/2,

[1] These authors contributed equally to this work.

[2] Correspondence: C.R.W.K., University Medical Center of the Johannes Gutenberg University Mainz, Institute of Physiology and Pathophysiology, Duesbergweg 6, 55131 Mainz, Germany. E-mail: kuhlma@uni-mainz.de; A.W., University Medical Center of the Johannes Gutenberg University Mainz, 1st Medical Department, Obere Zahlbacherstr. 63, Verfügungsgebäude, 55128 Mainz, Germany. E-mail: waisman@uni-mainz.de

doi: 10.1096/fj.09-141978

heme oxygenase 1, and peroxiredoxin-1 in active demyelinating MS lesions and the EAE model is clearly associated with a loss of BBB integrity (17, 18).

The aim of the present study was to investigate the mechanism underlying IL-17A-induced BBB disruption and the subsequent inflammatory activation of BECs. We demonstrate that IL-17A increased the production of ROS in BECs. The resulting oxidative stress mediates activation of the endothelial contractile machinery. Activation of the contractile apparatus is responsible for the loss and disorganization of TJ proteins, which consecutively lead to BBB breakdown. Furthermore, ROS production results in an up-regulation of endothelial adhesion molecules and an augmented adhesion and transmigration of inflammatory cells through the BBB.

MATERIALS AND METHODS

Cell culture

Immortalized BALB/C BECs [bEnd.3; American Type Culture Collection (ATCC), Manassas, VA, USA] were used as a BBB model as described previously (19). Cells were grown in culture flasks (TPP, Trasadingen, Switzerland). Medium consisted of DMEM GlutaMAX, supplemented with 2% penicillin/streptomycin and 15% FCS (all from Invitrogen, Karlsruhe, Germany). Medium was exchanged every 48 h, and cells were split once a week and afterward seeded 1:10 in a new flask. For experiments, cells were grown to confluence on 96-well plates with electrical cell impedance sensing (ECIS) electrode arrays and for transmigration on 24-well filter insert plates, respectively (Greiner Bio One, Solingen, Germany). For inflammation assays, the murine monocytotic cell line JAWSII (ATCC) was used. Cells were cultured in culture flasks using modified essential medium-α supplemented with 15% FCS and 5 ng/ml granulocyte-macrophage colony-stimulating factor (GM-CSF) (all from Invitrogen). Medium was added every 72 h, and cells were split to a factor of 1:5 once a week. All cells were kept in an incubator (New Brunswick Scientific, Nürtingen, Germany) at a CO_2 fraction of 5% and at 37°C.

Substances and chemicals

Recombinant mouse IL-17A and IL-22 was purchased from Sigma (Deisenhofen, Germany) and used in a range from 1 to 100 ng/ml. The following inhibitors were used: allopurinol (Allo; 500 μM), acetylsalicylic acid (ASS; 100 μM) (both Sigma), *N*-monomethyl-L-arginine (L-NMMA; 300 μM), 1-(5-iodonaphthalene-1-sulfonyl)-1*H*-hexahydro-1,4-diazepine hydrochloride (ML-7; 10 μM), and diphenyleneiodonium (DPI; 5 μM) (all from Calbiochem, Darmstadt, Germany).

For resistance measurements, the following substances were used: 1,2-bis(2-aminophenoxy)ethane tetraacetic acid (BAPTA; 10 μM) (Calbiochem), *N*-acetyl-L-cysteine (NAC; 10 μM) (Sigma), anti-IL-17 antibody (IL-17A; 20 ng/ml), and nonfunctional isotype control antibody (BioLegend, San Diego, CA, USA). In all experiments, drugs were added to the cells at least 30 min before stimulation with IL-17A. All chemicals were dissolved in water except ML-7, DPI, and BAPTA, which were solved in DMSO. The amount of DMSO in the final solutions was <0.01%. All vehicle controls were performed using water or DMSO. No significant changes were observed between water- and DMSO-treated controls. Hydroethidine (HE), Evans blue (EB), and trichloroacetic acid (TCA) were obtained from Sigma. Fluorescein-conjugated *Lycopersicon esculentum* (tomato) lectin (FITC-LEA) was from Vector Laboratories (Burlingame, CA, USA). The CyQuant DNA staining kit was purchased from Invitrogen.

ROS measurements

Confluent BECs were stimulated with IL-17A in a time (1–24 h)- and concentration (1–100 ng/ml)-dependent manner. IL-17A was diluted to the desired concentration using culture medium and then directly added to the wells. The generation of ROS was measured using 2′,7′-dichlorodihydrofluorescein (DCFH) (Sigma), which is oxidized to fluorescent dichlorofluorescein (DCF) in the presence of ROS. DCFH was used in a concentration of 10 μM and diluted in HBSS (Invitrogen), supplemented with glucose (10 mM), $CaCl_2$ (2 mM), and $MgCl_2$ (1 mM) ($HBSS^{+++}$, all from Merck, Darmstadt, Germany). Cells were incubated with the dye for 30 min. After incubation, the dye was removed and replaced by $HBSS^{+++}$, fluorescence was measured immediately at an excitation wavelength of 485 nm and an emission wavelength of 535 nm using an infinite F200 Tecan Microplate Reader, and data were acquired using i-control software (both from Tecan Trading AG, Männedorf, Switzerland). *In vivo* detection of ROS was performed using the superoxide-sensitive fluorescent dye HE. HE is oxidized by superoxide to dihydroethidine (DHE). Then 200 μl of a 1 μg/ml HE solution was injected i.p. 15 min before animals were sacrificed. Tissue was homogenized as described previously (20) and costained with CyQuant DNA stain. DHE fluorescence was measured using the above-mentioned plate reader (excitation 540 nm; emission 595 nm) and set in relation to the amount of DNA in the homogenate. To detect superoxide *in situ* in BECs, animals received an additional i.p. injection of FITC-LEA (100 μg in 50 μl of PBS). After homogenization, spinal cord tissue was analyzed by FACS scans as described in more detail by Benton *et al.* (20). DHE fluorescence (in relative fluorescence units) was quantified in the DHE- and FITC-LEA-positive cell population.

Resistance measurements

Endothelial monolayer resistance was monitored with the ECIS method using the ECIS 1600 instrument and 8W10E electrode arrays. All equipment was purchased from ibidi GmbH in cooperation with Applied BioPhysics (Martinsried, Germany). Cells were grown on 8-well electrode arrays, and IL-17A or IL-22 (1–100 ng/ml), NAC, BAPTA, ML-7, DPI, Allo, and anti-IL-17A were added in the above-mentioned concentrations when cells were confluent, showing a stable plateau of resistance value on a connected monitor. Data are expressed as relative changes of resistance values.

Cell viability

To examine possible cytotoxic effects of IL-17A, an Alamar blue assay was performed. bEnd.3 cells were grown to confluence in 96-well plates and treated for 24 h with 1, 10, 50, or 100 ng/ml IL-17A. After this incubation period, IL-17A was removed, and the cells were incubated in 100 μl of $HBSS^{+++}$ supplemented with Alamar blue dye in a dilution of 1:60 for 4 h. Absorption was measured at 595 nm using the above-mentioned microplate reader. Values were set in relation to untreated controls.

In-cell Western blot analysis

In-cell Western blot analysis was used to investigate the expression of the TJ proteins zonula occludens-1 (ZO-1) and occludin, the phosphorylated myosin light chain (pMLC), and endothelial adhesion molecules [intercellular adhesion molecule (ICAM-1), vascular cell adhesion molecule (VCAM-1), E-selectin, and P-selectin]. bEnd.3 cells were stimulated with 100 ng/ml IL-17A for 0.25 to 24 h. In some experiments, Allo, DPI, and ML-7 were used. After completion of IL-17A incubation, IL-17A-containing medium was removed, and cells were fixed with 4% formaldehyde (Roth, Karlsruhe, Germany). After 20 min, fixing solution was removed, and cells were permeabilized using Triton washing solution [0.1% Triton X-100 (Sigma) in 1× PBS (Invitrogen)] for 20 min. After removal of the Triton solution, cells were blocked with 1× PBS containing 10% FCS (blocking buffer) for 1.5 h. Primary antibodies (all from Santa Cruz Biotechnology, Inc., Heidelberg, Germany) were diluted (1:100 in blocking buffer), added to the wells, and incubated for 2 h. Corresponding biotinylated secondary antibodies (diluted 1:800 in blocking buffer) (all from Sigma) were added for 1 h after the cells were washed 4 times with Tween 20 washing solution [0.1% Tween 20 (Sigma) in 1× PBS]. Cells were finally marked with a fluorescent DNA dye (SYTO Green; Invitrogen) and a different fluorescent dye connecting to the secondary antibody (Cy3-streptavidin; Jackson ImmunoResearch Laboratories Inc., West Grove, PA, USA). After 1 h of incubation, dyes were washed out, and fluorescence was measured immediately.

Immunohistochemistry

bEnd.3 cells were grown to confluence on glass coverslips. After incubation with 100 ng/ml IL-17A for 24 h, cells were fixed for 20 min using 4% paraformaldehyde. Fixing solution was removed and cells were permeabilized using Triton washing solution (0.1% Triton X-100 in 1× PBS)) for 20 min. After removal of the Triton solution, cells were blocked with 1× PBS containing 10% FCS (blocking buffer) for 1.5 h. Primary antibodies against occludin and ZO-1 were used in the concentrations mentioned above and were incubated at 4°C overnight. After washing, biotinylated secondary antibodies were added and incubated for 1 h. Thereafter, Cy3-streptavidin was added to stain either ZO-1 or occludin for 1 h. After washing, the coverslips were mounted on microscope slides using Fluoromount medium (SouthernBiotech, Birmingham, AL, USA). Staining of cells with the secondary antibody served only as a negative control. Immunocytochemistry in spinal cord sections of EAE mice was performed as follows. Mice were perfused with an ice-cold solution containing 4% paraformaldehyde in phosphate buffer. Spinal cords were dissected and cut into 70-μm-thin sections using a Vibratome. Slices were washed and blocked (10% normal serum and 0.5% Triton X-100) before overnight incubation with rabbit anti-ICAM-1, anti-mouse IgG (1:100; Santa Cruz Biotechnology, Inc.), anti-pMLC, and/or CD31 (both 1:100; Sigma) antibody. Sections were immunostained using FITC-labeled secondary antibodies. Pictures were made using an upright microscope (BX51WI; Olympus, Hamburg, Germany), equipped with a Nipkow spinning disk confocal system (QLC10; Visitech, Sunderland, UK) and a krypton/argon laser (LaserPhysics, Cheshire, UK). For comparison, pictures of different groups were all taken using the same exposure time. Fluorescence intensities of IgG stainings were measured in the total field of view (×20), whereas pMLC fluorescence intensity was analyzed in defined regions of interest of CD31-pMLC double-labeled microvessels (×60). Fluorescence intensities are given as relative fluorescence units.

Monocyte adhesion and transmigration

bEnd.3 cells were stimulated with 100 ng/ml IL-17A for 1 to 24 h. JAWSII cells were harvested, washed with RPMI 1640 medium (Invitrogen), and incubated with 1 μM calcein red AM dye (Invitrogen) for 30 min. Cells were then washed 2 times with RPMI 1640 and diluted to a concentration of 2×10^6 cells/ml. IL-17A-containing medium was removed from bEnd.3 cells. JAWSII cells were added and incubated with endothelial cells for 1 h. The wells were then washed 3 times with $HBSS^{+++}$ to remove nonadherent monocytes. $HBSS^{+++}$ was added for measurement. Plates were measured at an excitation wavelength of 540 nm and emission wavelength of 585 nm.

For monocyte transmigration, bEnd.3 cells were grown to confluence in the upper chamber of 3-μm-pore fluorescence blocking filters inserted in 24-well plates (BD FluoroBlok; Falcon; BD Biosciences Discovery Labware (Bedford, MA, USA). Barrier function in these monolayers was checked by transepithelial electrical resistance (TEER) measurements with a chopstick electrode that was connected to an epithelial ohmmeter (all devices were from World Precision Instruments, Berlin, Germany). The resistance of blank filters was subtracted as background resistance from the total resistance of each culture insert. TEER values were in the range of $127.6 \pm 31.5\ \Omega\ cm^2$. To examine whether astrocytic factors influence TEER values, the culture medium was supplemented with astrocyte-conditioned medium, as described in more detail previously (21). TEER values were not significantly enhanced by astrocyte-conditioned medium ($131.8 \pm 23.7\ \Omega\ cm^2$; $n=12$; NS, astrocyte-conditioned *vs.* not conditioned culture medium). For transmigration experiments only filters with resistance values $>100\ \Omega\ cm^2$ were used. Monocytes were treated and dye-labeled as mentioned above and added to the upper chamber of the filter. The plate was then positioned in the fluorescence reader, and measurement was started. IL-17A (1, 10, 50 and 100 ng/ml) was added after 10 min to the upper compartment. Fluorescence measurements were taken from the bottom of the wells; because of the fluorescence-blocking properties of the filters, only the fluorescence from transmigrated monocytes was captured. Fluorescence of IL-17A-treated filters was set in relation to the vehicle-treated control.

Induction and clinical evaluation of EAE

EAE was induced in 6- to 12-wk-old female C57BL/6 wild-type (WT) or IL-17A$^{-/-}$ mice by injecting 50 μg of MOG_{35-55} peptide (MEVGWYRSPFSRVVHLYRNGK) in complete Freund's adjuvant (CFA) (Sigma) supplemented with 8 mg/ml heat-inactivated *Mycobacterium tuberculosis* (H37Ra strain; Difco Laboratories, Detroit, MI, USA) on d 0 in the tail base. *Bordetella pertussis* toxin (200 ng; Sigma) was administered i.p. on the day of immunization and 2 d later. Between d 3 and 12, mice were injected i.p. every 12 h with the myosin light chain kinase (MLCK) inhibitor ML-7 (Biomol Research Laboratories, Plymouth Meeting, PA, USA) (2 mg/kg body weight in PBS). Control animals were injected with PBS. Mice were monitored daily for clinical signs of EAE, graded on a scale from 0 to 6 as follows: 0, clinically normal; 1, loss of tail tonicity; 2, impaired righting reflex on attempt to roll over; 3, hindlimb paresis; 4, hindlimb paralysis; 5, forelimb paresis; and 6, dead animal. Mice were sacrificed at d 20 after disease induction at varying clinical scores to obtain inflammatory CNS infiltrates, which were isolated using a Percoll (Life Technologies, Inc., Carlsbad, CA, USA) gradient as described previously (22).

Cells were surface-stained with anti-CD45, IFN-γ (BD, Franklin Lakes, NJ, USA), and anti-CD11b (homemade). Intracellular staining was performed on *ex vivo* CNS-derived cells using Cytofix/Cytoperm (BD) according to the manufacturer's recommendations. Th17 intracellular stainings were performed using an allophycocyanin (eBioscience, San Diego, CA, USA) or phycoerythrin-conjugated anti-IL-17A antibody (BD).

EB extravasation

As a marker of BBB disruption *in vivo*, animals received an i.p. injection of EB (1 ml of 0.4% EB in PBS) 24 h before sacrifice. After transcardial perfusion brain and spinal cord were removed, weighed, and stored at −80°C. Each hemisphere and the spinal cord were homogenized in 1 ml of 50% TCA. After centrifugation, EB fluorescence was measured at an excitation of 620 nm and an emission wavelength of 680 nm.

Real-time PCR

Total RNA from spinal cord was purified using TRIzol RNA isolation reagent (Invitrogen Life Technologies) according to the manufacturer's protocol. The RNA was cleaned further using an RNeasy Mini Kit (Qiagen, Hilden, Germany). Then 1 μg of total RNA was reverse-transcribed using the Transcriptor High Fidelity cDNA Synthesis Kit (Roche Applied Science, Mannheim, Germany) according to the manufacturer's protocol using random hexameric primers. cDNA was amplified with the LightCycler TaqMan Master Kit (Roche Applied Science) and analyzed with the LightCycler 1.5 capillary-based system (Roche Applied Science) using the Universal ProbeLibrary (Roche Applied Science) for detection. The primers and probes were designed with the help of the Roche Applied Science website-based Universal ProbeLibrary Assay Design Center. β-Actin (ACTB) was used as a reference gene. The following primers were used: IL-17A, 5′-CAGGGAGAGCTTCATCTGTGT-3′ and 5′-GCTGAGCTTTGAGGGATGAT-3′, probe no. 74; IL-22, 5′-TTTCCTGACCAAACTCAGCA-3′ and 5′-TCTGGATGTTCTGGTCGTCA-3′, probe no. 17; GM-CSF, 5′-GCATGTAGAGGCCATCAAAGA-3′ and 5′-CGGGTCTGCACACATGTTA-3′, probe no. 79; IL-22 receptor 1 (IL-22R1), 5′-CTGTGCAGGGGTCCAGAG-3′ and 5′-TGAAGGAGACCGGATGTGT-3′, probe no. 81; and ACTB, 5′-TGACAGGATGCAGAAGGAGA-3′ and 5′-CGCTCAGGAGGAGCAATG, probe no. 106.

Dilution series of target and reference genes were quantified by PCR and imported into the LightCycler Relative Quantification Software (Roche Applied Science) to obtain concentration ratios of target and reference genes from experimental samples. Conventional relative quantification (ΔΔCt method) could not be performed because some of the target mRNAs could not be detected in samples from unimmunized or ML-7-treated animals owing to the low expression rate in these cases.

Conventional RT-PCR

Total RNA from 2×10^6 bEnd.3 cells was extracted using an RNeasy Mini Kit (Qiagen). Then 1 μg of total RNA was reverse-transcribed using SuperScript II reverse transcriptase (Invitrogen Life Technologies) according to the manufacturer's protocol with oligo$(DT)_{12–18}$ primer. cDNA was amplified with the following primers specific for IL-17A or IL-22R1: IL-17RA, 5′-GCAGCTGAACACCAATGAGC-3′ and 5′-GCAGCACCAGTGAAACTTGC-3′ and IL-22R1, 5′-CCAGCGGATCACCCAGAAGT-3′ and 5′-ATCGGGCAGCGTCTTCACTC-3′. Glyceraldehyde-3-phosphate dehydrogenase was used as a reference gene (5′-ACCACAGTCCATGCCATCAC-3′ and 5′-TACAGCAACAGGGTGGTGGA-3′).

Statistical analysis

Results are represented as mean ± SE [SCAP] values. Statistical analysis was performed by ANOVA and *post hoc* Tukey tests using GraphPad Prism (Windows version 4.02; GraphPad Software, San Diego, CA, USA).

RESULTS

IL-17A-induced BBB disruption involves down-regulation and reorganization of TJ molecules

Th17 cells, which produce the cytokines IL-17A, IL-17F, and IL-22, were shown to infiltrate the CNS in patients with MS and in mice with EAE (23, 24). Recently, it was shown that both IL-17A and IL-22 can disturb BBB integrity, but the exact mechanism by which this occurs is not clear (5). To test how IL-17A influences BBB integrity, we used the cell culture model of bEnd.3 monolayer cells. To analyze the influence of IL-17A on the integrity of the bEnd.3 monolayer, recombinant IL-17A was used. The cytokine in concentrations of 1, 10, 50, and 100 ng/ml was added to an intact bEnd.3 monolayer grown on an ECIS array. The electrical resistance of the bEnd.3 monolayer is proportional to the endothelial monolayer integrity, and therefore the BBB integrity can be monitored continuously using ECIS technology. After reaching a stable electrical resistance level, the bEnd.3 monolayer was stimulated with IL-17A. IL-17A caused a time-dependent decrease of the relative electrical resistance values at a concentration of 100 ng/ml. Lower concentrations of IL-17A (1–50 ng/ml) had no effect on barrier function (Supplemental Fig. 1*A*). The barrier-disrupting effect reached a maximum after 7 h of IL-17A incubation. To examine whether the effect of IL-17A is not due to unspecific side effects of the recombinant protein, we treated bEnd.3 cells with an IL-17A-neutralizing antibody. This antibody completely blocked the barrier-disrupting effect of IL-17A, whereas an isotype control antibody did not affect IL-17A-induced barrier disruption (**Fig. 1*A***). Furthermore, we wanted to exclude the possibility that the barrier-disrupting effect of IL-17A was due to the cytotoxic effects of IL-17A. Cell viability was analyzed using an Alamar blue viability assay, but we found no effect on cell viability of IL-17A at concentrations up to 100 ng/ml (Supplemental Fig. 1*B*). Next we examined whether IL-22 shows similar effects on barrier function. To our surprise, IL-22 did not induce barrier disruption in bEnd.3 monolayers (Supplemental Fig. 2). To further analyze this finding, we examined whether IL-22 receptors are expressed on bEnd.3 cells. As shown in Supplemental Fig. 3*A*, IL-22 receptor expression could not be detected by quantitative real-time PCR. In contrast, we were able to show IL-17A receptor expression (Supplemental Fig. 3*B*).

TJ proteins play a pivotal role in maintaining BBB

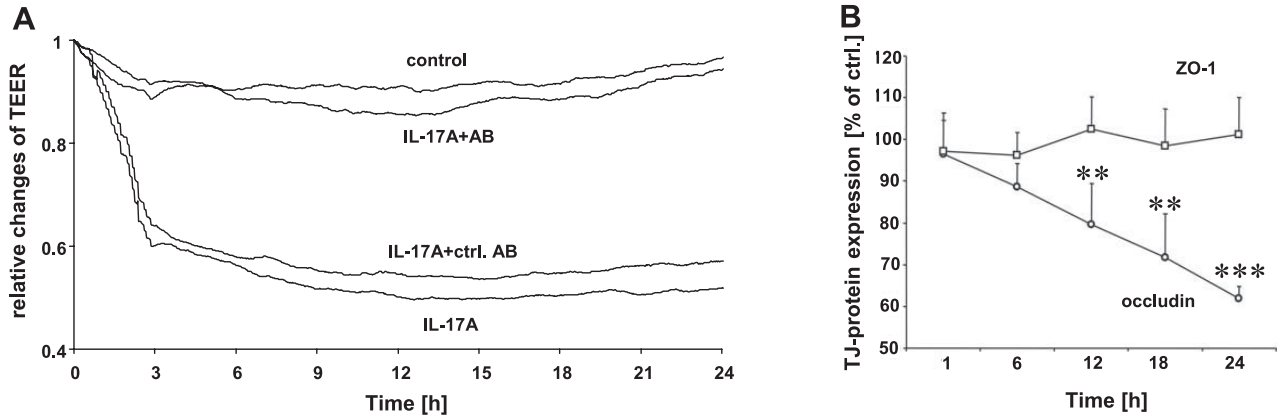

Figure 1. IL-17A impairs BBB integrity involving TJ modulation. *A*) Representative ECIS measurements show the 100 ng/ml IL-17A-induced decrease of relative TEER values that was blocked by an IL-17A-neutralizing antibody (20 ng/ml; IL-17A+AB). A nonfunctional control antibody (20 ng/ml; IL-17A+ctrl. AB) had no effect on IL-17A-induced barrier disruption. *B*) TJ protein occludin shows a lower expression on endothelial cells treated with 100 ng/ml IL-17A, as shown by an in-cell Western assay (61.84±3.05% of untreated control after 24 h). TJ protein ZO-1 is not afflicted; $n=3$ independent experiments. $^{**}P < 0.01$; $^{***}P < 0.001$. *C*) Immunohistochemical analysis shows altered ZO-1distribution (arrows) in 100 ng/ml IL-17A-treated cells (×20).

integrity. Down-regulation and disorganization of TJ molecules are central factors responsible for BBB disruption. For this reason we examined the effect of IL-17A on the protein expression and organization of the TJ molecules occludin and ZO-1 using the in-cell Western blot technique and analyzed immunostainings using confocal laser scanning microscopy. IL-17A (100 ng/ml) treatment for 24 h caused a time-dependent down-regulation of occludin, whereas ZO-1 protein levels were not affected (Fig. 1*B*). The immunostainings of ZO-1 showed a strong disturbance of ZO-1 organization at the cell borders of bEnd.3 cells after IL-17A treatment (Fig. 1*C*). These findings indicate that the IL-17A-induced barrier-disrupting effects of these TJ molecules occur at the protein expression level (occludin) and at the subcellular localization (ZO-1).

Mechanisms mediating IL-17A effects on BEC permeability

Previous observations indicated that BBB disruption involves the activation of the endothelial contractile machinery, elevation of intracellular calcium levels, and the generation of ROS (14, 16, 25, 26). We performed further ECIS measurements to examine which of these mechanisms are involved in IL-17A-induced BBB disruption. As shown in **Fig. 2*A***, addition of the ROS scavenger NAC prevented the barrier-disrupting effect of IL-17A, demonstrating the involvement of ROS production. To further study the role of ROS, intracellular ROS levels were analyzed in bEnd.3 cells by microplate fluorescence reading using the ROS-detecting fluorescent dye DCF. Common enzymatic sources of ROS in endothelial cells are NAD(P)H oxidase, cyclooxygenase, xanthine oxidase, and endothelial nitric oxide synthase (eNOS) (27). We found that IL-17A induced a time- and concentration-dependent increase of ROS formation in bEnd.3 cells (Fig. 2*B*). IL-17A-induced oxidative stress reached a maximum at a concentration of 100 ng/ml after an incubation period of 12 h (Fig. 2*C*). To identify the ROS-producing enzyme that is activated by IL-17A, bEnd.3 cells were pretreated with inhibitors directed against xanthine oxidase (Allo; 500 μM), cyclooxygenase (ASS; 100 μM), NAD(P)H oxidase (DPI; 5 μM), and eNOS (L-NMMA; 300 μM). Inhibitors of NAD(P)H oxidase and xanthine oxidase completely abolished the effect of IL-17A, whereas L-NMMA and ASS had no effect the IL-17A-induced ROS formation, indicating that the NAD(P)H and xanthine oxidase are involved in IL-17A-induced oxidative stress.

The endothelial contractile machinery is strongly regulated by the phosphorylation of myosin light chains (MLCs) (28). The MLC phosphorylation state is controlled by MLCK kinase and MLC phosphatase (29, 30). Because we and others previously demonstrated that prevention of MLC phosphorylation preserves BBB integrity, we examined whether the MLCK inhibitor ML-7 can prevent IL-17A-induced BBB disruption. As demonstrated in Fig. 2*A*, ML-7 completely abolished the barrier-disrupting effect of IL-17A in BECs. To further study this effect, we directly analyzed the MLC phosphorylation level in BECs using the in-cell Western blot technique. IL-17A caused a time-dependent in-

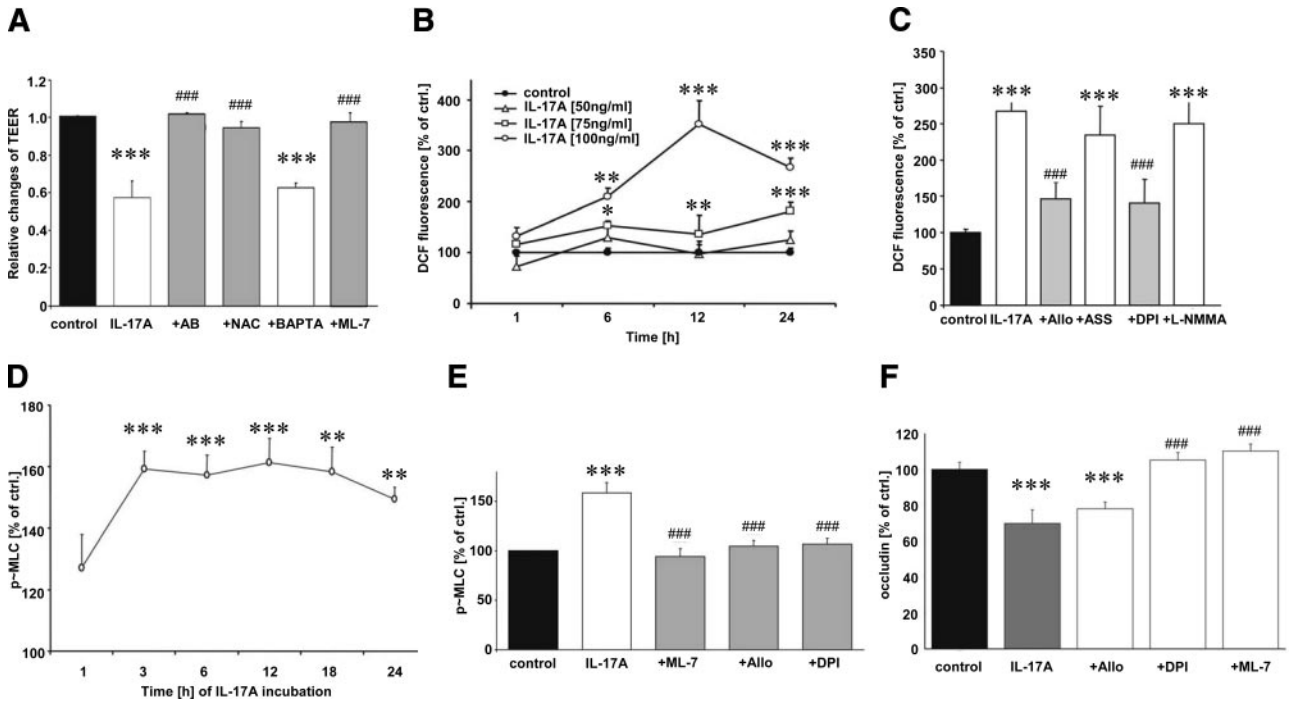

Figure 2. Mechanisms involved in IL-17A actions. *A*) Neutralizing IL-17A as well as scavenging ROS (NAC; 1 mM) but not chelating calcium (BAPTA; 10 μM) prevented the 100 ng/ml IL-17A-induced TEER decrease in ECIS measurements. Inhibition of MLCK with ML-7 (10 μM) also avoided BBB breakdown (n=6). *B*) IL-17A-induced time- and concentration-dependent increases in ROS production, as shown by DCF fluorescence measurements (maximum after 12 h at 100 ng/ml IL-17A: 351.57±18.33% of control; n=6). *C*) The 100 ng/ml IL-17A-induced ROS production in BECs depends on NADPH (DPI; 5 μM) oxidase and xanthine oxidase (Allo; 500 μM) activation, whereas cyclooxygenase (ASS; 100 μM) and NO-synthase (L-NMMA; 300 μM) are not involved (n=12). *D*) Time course of MLC phosphorylation induced by IL-17A (100 ng/ml). *E*) IL-17A-induced up-regulation of pMLC demonstrates the participation of the contractile machinery in BBB breakdown (158.31±10.61% of untreated control after 3 h of IL-17A incubation; n=4). This activation of the contractile machinery could be blocked using DPI (5 μM), Allo (500 μM), and ML-7 (10 μM) (n=4). *F*) Blocking either MLCK with ML-7 (10 μM) or NADPH oxidase with DPI (5 μM) prevents IL-17A-induced down-regulation of occludin (n=4). $^{**}P < 0.01$, $^{***}P < 0.001$ *vs.* control; $^{\#\#\#}P < 0.001$ *vs.* IL-17A.

crease in pMLC, reaching a plateau after 3 h that lasted up to 24 h of IL-17A treatment (Fig. 2*D*). As expected, the MLCK inhibitor ML-7 completely blocked the IL-17A-induced increase of pMLC. Furthermore, the inhibitors of xanthine oxidase and NAD(P)H oxidase prevented IL-17A-induced pMLC, indicating that the effect of IL-17A on the endothelial contractile machinery is mediated *via* ROS (Fig. 2*E*). Previously we were able to demonstrate that hypoxia-induced BBB disruption is blocked by ML-7 and that the hypoxia-dependent elevation of pMLC in bovine BECs is completely abolished by blocking NAD(P)H oxidase-induced ROS generation (14). Similar results were obtained by Haorah et al (26), demonstrating that ethanol-induced BBB disruption involves a ROS-dependent activation of the MLCK. Interestingly, we could not observe a protective effect of the calcium chelator BAPTA, indicating that in contrast to our previous observation under acute hypoxia (14), calcium signaling is not involved in the barrier-disturbing effect of IL-17A (Fig. 2*A*).

Because we have demonstrated that IL-17A down-regulates the protein expression of the TJ molecule occludin, we next investigated the involvement of ROS signaling or the activation of MLCK. The NAD(P)H oxidase inhibitor DPI and the MLCK inhibitor ML-7 completely abolished the effect of IL-17A on occludin expression. However, the xanthine oxidase inhibitor Allo failed to block the effect of IL-17A (Fig. 2*F*), indicating that NAD(P)H oxidase and not xanthine oxidase is responsible for the decrease in occludin protein levels. A possible explanation is given by the subcellular localization of both enzymes. Xanthine oxidase is located in the cytoplasm, whereas activated NAD(P)H oxidase is embedded in the cell membrane. Therefore, NAD(P)H oxidase-derived ROS can easily degrade the TJ molecules in their close vicinity, whereas radicals produced by xanthine oxidase can be neutralized by intracellular ROS-defending systems such as the glutathione system.

IL-17A induces an inflammatory response in bEnd.3 cells

Monocyte adhesion and transendothelial migration are key features of the inflammatory response in MS and EAE. Therefore, we addressed the question of whether IL-17A induces the adhesion and transmigration of the murine monocytotic cell line JAWSII. We found that incubation with IL-17A caused an increase of JAWSII

cell adhesion with a peak after 3 h (**Fig. 3*A***). The contribution of ROS to IL-17A-induced monocyte adhesion could be verified by adding the respective inhibitors. Similar to the results of the DCF experiments, DPI (5 μM) and Allo (500 μM) completely blocked IL-17A-induced monocyte adhesion, whereas ASS (100 μM) and L-NMMA (300 μM) had no effect (Fig. 3*B*). Because monocyte adhesion is strongly correlated with the expression of adhesion molecules on BECs, we examined whether IL-17A affects the expression of ICAM-1, VCAM-1, P-selectin, or E-selectin using the in-cell Western blot technique. Indeed, IL-17A treatment increased the expression of ICAM-1, but expression of P-selectin, E-selectin, and VCAM-1 remained unaffected (Fig. 3*C*).

The adhesion of monocytes to bEnd.3 cells is the initial step, which is required for the recruitment of these cells to the inflammation sites in the CNS, as occurs in MS and EAE (31). After the monocytes adhere, they transmigrate through the endothelial cells into the subendothelial space, reaching the neuronal and glial cells, and cause the characteristic tissue destruction (*e.g.*, demyelination) (32, 33). In addition, loss of BBB integrity, *e.g.*, by destruction of the TJ molecules, is required to support the transendothelial migration (34). Therefore, we examined whether IL-17A enhances JAWSII cell transendothelial migration. For this purpose, bEnd.3 cells were seeded on fluoro-block filters that allow a continuous examination of fluorescent (calcein red AM)-labeled JAWSII cell transendothelial migration. As illustrated in Fig. 3*D*, IL-17A treatment induced a continuously increasing JAWSII cell transmigration, reaching a plateau-like maximum after 20 h. The IL-17A-induced transendothelial migration was significantly reduced by inhibitors of NAD(P)H oxidase, xanthine oxidase, or MLCK (Fig. 3*E*).

Prevention of BBB destruction by MLCK inhibition ameliorates autoimmune brain inflammation

We have shown that IL-17A induces phosphorylation of MLC in BECs, which in turn leads to the permeability increase of the BBB cells. Next, we were interested in testing whether such a mechanism of BBB permeabilization may also influence the influx of cells during autoimmune brain inflammation. This information is most relevant for understanding the action mode of IL-17A, because it was shown recently that Th17 cells are found in the CNS of patients with MS and that the receptors for IL-17A and IL-22 are expressed on the surface of the BBB endothelial cells (5). To test whether the IL-17A-dependent activation of the endothelial contractile machinery is also responsible for BBB destruction and the induction of autoimmunity *in vivo*, we used the murine model of MS, EAE. A correlative link between IL-17A expression and the development of EAE has been well documented, as Th17 cells are abundant in the CNS of mice before and during the peak of the disease (35). To inhibit the IL-17A-mediated activation of the endothelial contractile machinery, we used the drug ML-7, which we have shown to be effective in culture (see Fig. 2*A*). ML-7 was shown to be active *in vivo* and to be devoid of toxic effects (14). We

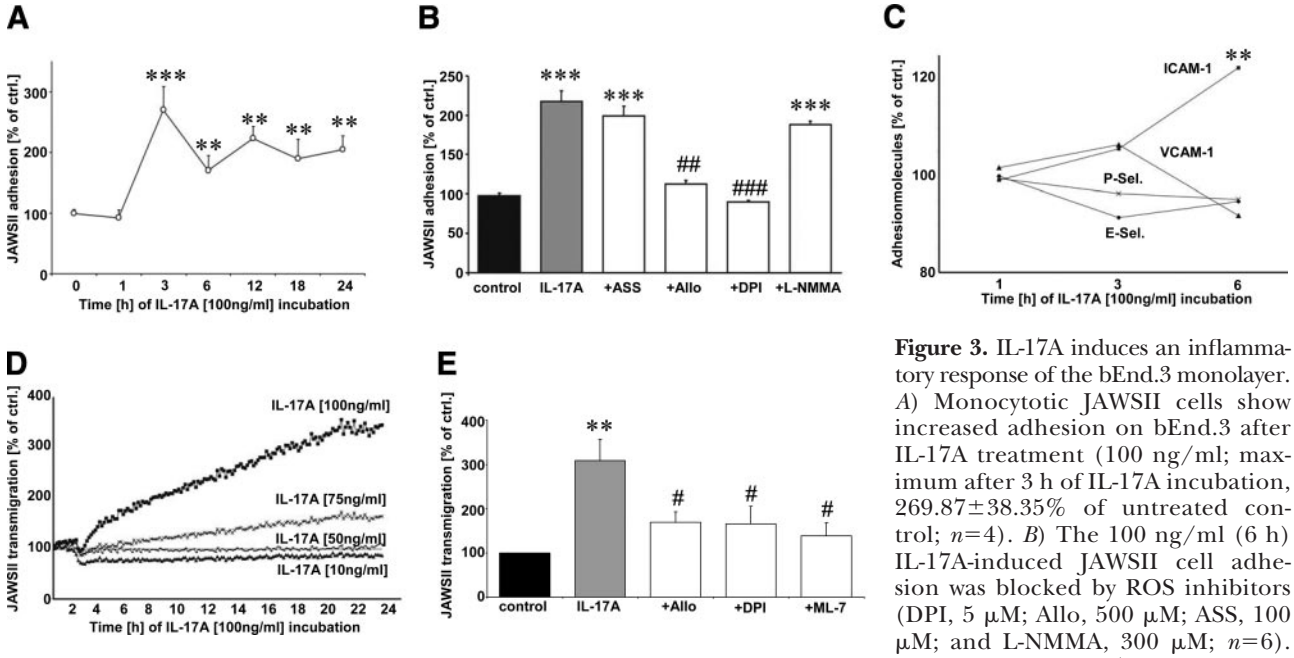

Figure 3. IL-17A induces an inflammatory response of the bEnd.3 monolayer. *A*) Monocytotic JAWSII cells show increased adhesion on bEnd.3 after IL-17A treatment (100 ng/ml; maximum after 3 h of IL-17A incubation, 269.87±38.35% of untreated control; $n=4$). *B*) The 100 ng/ml (6 h) IL-17A-induced JAWSII cell adhesion was blocked by ROS inhibitors (DPI, 5 μM; Allo, 500 μM; ASS, 100 μM; and L-NMMA, 300 μM; $n=6$). *C*) Adhesion molecule ICAM-1 was up-regulated significantly when the bEnd.3 was treated with IL-17A (100 ng/ml; 122.42±5.33% of untreated control; 6 h). VCAM-1, P-selectin (P-Sel.), and E-selectin (E-Sel.) expression was not influenced by IL-17A ($n=3$). *D*) IL-17A also enhanced monocytotic transmigration through the confluent endothelial cells in a concentration-dependent manner (top trace, 100 ng/ml IL-17). *E*) The 100 ng/ml (24 h) IL-17A-induced transmigration could be blocked by inhibition of NADPH (DPI, 5 μM), xanthine oxidase (Allo, 500 μM), or MLCK (ML-7 10 μM) ($n=6$). $^{**}P<0.01$, $^{***}P<0.001$ *vs.* control; $^{\#}P<0.05$, $^{\#\#}P<0.01$, $^{\#\#\#}P<0.001$ *vs.* IL-17A.

used a concentration of 2 mg of ML-7/kg body weight, which was previously shown in Wistar rats to be effective in a stroke animal model (14). To induce EAE, mice were injected with the MOG peptide (p35–55) emulsified in CFA followed by two injections of pertussis toxin. This protocol normally leads to the development of clinical signs of EAE ~9–11 d after immunization of C57BL/6 mice. From d 3 to d 12 we treated immunized mice with ML-7 to prevent BBB destruction. As can be seen in **Fig. 4*A***, disease onset occurred at d 9. However, mice treated with ML-7 developed significantly milder clinical signs in the 1st week after disease onset. After the initial disease phase, vehicle-treated as well as ML-7-treated mice recovered, demonstrating that ML-7-treated mice exhibit a milder form of the disease, but otherwise with a course similar to that in the control mice.

Our hypothesis is that ML-7, by inhibiting the activation of the endothelial contractile machinery in BECs after triggering by IL-17, leads to lower infiltration of lymphocytes to the CNS. Because the pathogenesis of EAE is dependent on the influx of lymphocytes and monocytes into the CNS *via* the BBB, this hypothesis could explain the finding that ML-7-treated mice show a lower clinical disease score than the controls. To address whether treatment with ML-7 reduces lymphocyte influx into the CNS, we induced EAE in a new group of mice and sacrificed them 20 d after immunization. As can be seen in Fig. 4*B*, we found a reduced number of lymphocytes ($CD45.2^{high}CD11b^{-}$) infiltrating into the CNS of ML-7-treated mice compared with that in vehicle-treated mice (Fig. 4*C*). We also observed a reduction in the numbers of macrophages, which by the secretion of proinflammatory cytokines and chemokines are thought to be critical for the manifestation of EAE. Finally, we investigated the ratio between Th1 *vs.* Th17 cells in the CNS of the treated mice. As can be seen in Fig. 4*B*, *C*, we found an overall reduction in the numbers of Th17 and Th1 cells in ML-7-treated mice compared with those in control mice. The effects of ML-7 also became evident in immunohistochemical sections stained for IgG which penetrates areas of damaged BBB, pMLC and ICAM-1, a marker for activated microglia. Permeability of the BBB for IgG, pMLC, and activation of microglia were evident in control animals with EAE but were clearly suppressed in ML-7-treated animals (Fig. 4*D* and **Table 1**). EB extravasation was analyzed as an additional marker of BBB disruption. As demonstrated in Table 1, EB extravasation and pMLC were increased in immunized mice, and this effect was significantly reduced in ML-7-treated mice. Furthermore, quantitative real-time PCR experiments were performed to examine whether ML-7 affects the expression levels of the major Th17 cytokines IL-17A, IL-22, and GM-CSF. The expression of all three cytokines in spinal cords of animals with EAE is up-regulated as shown in Fig. 4*E*. This up-regulation is suppressed by the treatment with ML-7, indicating that treatment with ML-7 results in reduced levels not only of EAE severity but also of pathogenic cytokines known to play a role in the disease.

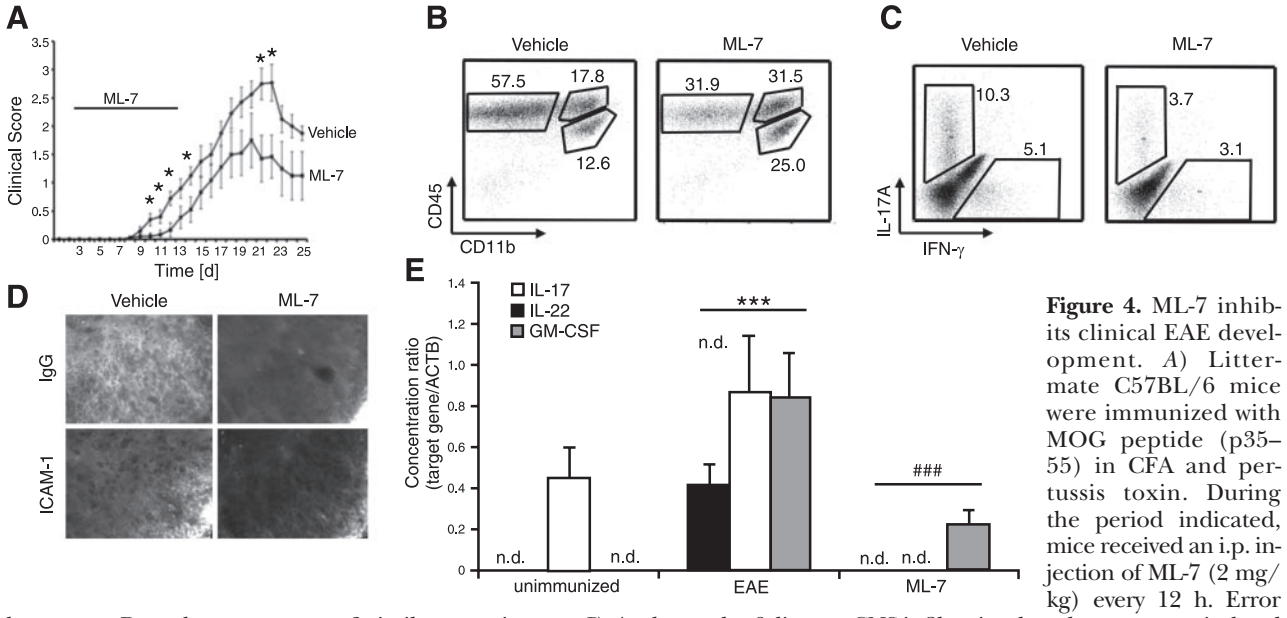

Figure 4. ML-7 inhibits clinical EAE development. *A*) Littermate C57BL/6 mice were immunized with MOG peptide (p35–55) in CFA and pertussis toxin. During the period indicated, mice received an i.p. injection of ML-7 (2 mg/kg) every 12 h. Error bars = SD. Data shown represent 3 similar experiments. *B*) At the peak of disease, CNS-infiltrating lymphocytes were isolated from pooled brain and spinal cord homogenates. Percentages of cells are shown in the indicated gates. *C*) CNS-infiltrating lymphocytes (as in *B*) were restimulated and stained intracellularly for IL-17A and IFN-γ. Dot plots are pregated on $CD4^{+}$ T lymphocytes. Percentages of cells are given in the indicated gates. *D*) Fluorescent microscopic pictures of spinal cord stained for IgG to detect permeability of the BBB for ICAM-1 as a marker of microglial activation. Note the evident differences between untreated (left column) and treated (right column) animals. Images were taken using the same exposure time. *E*) ML-7 prevents the expression of Th17 cytokines in the spinal cord. cDNA of unimmunized mice, immunized mice (EAE), and immunized mice treated with ML-7 was analyzed by real-time PCR at the peak of disease. IL-17A, IL-22, and GM-CSF are up-regulated in mice afflicted EAE compared to unimmunized control animals (n=3). n.d., not determined. $^{***}P < 0.001$ *vs.* unimmunized; $^{\#\#\#}P < 0.001$ *vs.* EAE.

TABLE 1. *Role of pMLC in EAE-dependent BBB disruption*

Treatment	EB (RFU/mg tissue)	IgG (RFU/field of view)	pMLC (RFU/CD31 stained vessel)
Unimmunized	7,471 ± 1043	12.1 ± 2.48	163.1 ± 10.13
EAE	46,180 ± 3500***	47.8 ± 3.71***	273.2 ± 18.27***
EAE + ML-7	26,230 ± 3570##	25.5 ± 0.48###	169.3 ± 14.55###
Unimmunized + ML-7	ND	13.2 ± 0.48	143.2 ± 7.01
IL-17A$^{-/-}$	ND	23.7 ± 0.85	197.4 ± 10.94###

All data represent mean ± SE values of at least $n = 3$ animals. RLU, relative fluorescence units; ND, not determined. ***$P < 0.001$ *vs.* unimmunized; ##$P < 0.01$, ###$P < 0.001$ *vs.* EAE.

IL-17A$^{-/-}$ mice show lower levels of oxidative stress and BBB disruption

Because we have shown that IL-17A induces oxidative stress in BECs *in vitro,* we decided to analyze whether IL-17A-induced ROS formation is also relevant in the EAE *in vivo* model. Levels of oxidative stress were determined in BECs *in situ* by combined *in vivo* staining of endothelial cells (FITC-LEA) and superoxide (DHE). DHE fluorescence in FITC-LEA-positive cells was increased by 37.8% in immunized mice compared with that in unimmunized mice. The DHE fluorescence of the complete spinal cord homogenate was increased by 98.4% in immunized compared with unimmunized mice. We further analyzed total DHE fluorescence intensity in the spinal cord homogenates of IL-17A$^{-/-}$ and WT mice. DHE fluorescence was significantly greater in immunized WT animals compared with animals that were unimmunized, whereas immunized IL-17A$^{-/-}$ mice showed lower levels of DHE fluorescence in the spinal cord (**Fig. 5**). Furthermore, pMLC and IgG stainings were more evident in immunized WT animals compared with IL-17A$^{-/-}$ mice (Table 1), indicating that the mechanism observed in the *in vitro* experiments also plays a role in the EAE *in vivo* model.

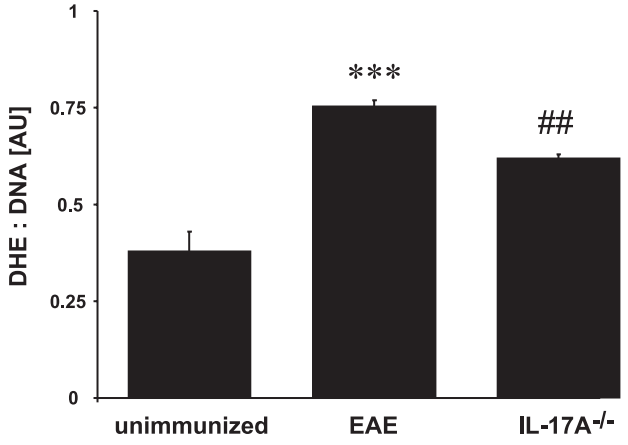

Figure 5. Prevention of EAE-induced BBB disruption in IL-17A$^{-/-}$ mice. Superoxide was stained in the spinal cord *in situ* by DHE. DHE fluorescence in spinal cord homogenates of WT and IL-17A$^{-/-}$ mice was set in relation to the respective fluorescence intensity of CyQuant DNA stain. Data are presented as quotient of DHE and CyQuant fluorescence in arbitrary units (AU); $n = 3$. ***$P < 0.001$ *vs.* EAE; #$P < 0.05$ *vs.* IL-17A$^{-/-}$.

DISCUSSION

The aim of the present study was to examine the mechanisms underlying IL-17A-induced BBB disruption in the pathogenesis of EAE and MS. We found that IL-17A-induced BBB disruption involves the formation of ROS by NAD(P)H oxidase and xanthine oxidase, which subsequently are responsible for the disruption and down-regulation of TJ molecules and the activation of the endothelial contractile machinery. We also found that monocyte adhesion and transmigration are enhanced by IL-17A treatment but that inhibition of MLC phosphorylation by treatment with ML-7 reduced lymphocyte and monocyte infiltration into the CNS, thus demonstrating a mechanism for IL-17A in BBB disruption *in vivo* during autoimmune disease.

IL-17A was recently implicated in the disruption of the BBB in a study performed by Kebir *et al.* (5). It was demonstrated that treatment with IL-17A or IL-22 increases the BSA permeability of human brain endothelial cells (HBECs). Further, the increased permeability was associated with a decrease in the expression of the TJ molecules occludin and ZO-1 in HBECs. Our present study using a murine BBB model is in good accordance with these observations. We found a plateau-like decrease of BBB integrity that was accompanied by decreased occludin expression. In contrast to the findings of Kebir *et al.* (5), we did not observe a down-regulation of total ZO-1 protein expression, but rather a disruption of the ZO-1 distribution pattern at the cell borders, suggesting that the IL-17A-induced BBB disruption involves modulation of the TJ molecules occludin and ZO-1. To our surprise, IL-22 had no effect on the murine BBB model. Using qRT-PCR, we were able to detect mRNA for IL-17A receptors, but not for IL-22 receptors in bEnd.3 cells. In addition, we used the far more sensitive quantitative real-time PCR method, but we were not able to detect the IL-22 receptor in bEnd.3 cells. Our data suggest the following signaling mechanism: IL-17A activates the endothelial IL-17A receptor, which is followed by increased ROS production mediated by NAD(P)H oxidase and xanthine oxidases. The resulting oxidative stress activates the endothelial contractile machinery by increasing the amount of phosphorylated MLC. Phosphorylated MLC interacts with the actin cytoskeleton, leading to a cell contraction that *per se* increases the intercellu-

lar space of the endothelial cell monolayer. In addition, we could show that the MLCK inhibitor ML-7 prevented the IL-17A-induced disruption of the TJ molecules, which further underlines the pivotal role of MLC phosphorylation in IL-17A-induced BBB disruption (**Fig. 6**).

We and others have demonstrated previously that ROS-induced activation of the endothelial contractile machinery leads to BBB disruption (14, 16, 26, 27, 36). Addition of exogenous ROS induced activation of the endothelial contractile machinery in a rat and human model of the BBB, resulting in barrier permeabilization (16, 26). Similar observations were made after induction of hypoxia (14) or treatment of HBECs with alcohol (37), which both resulted in NAD(P)H oxidase-dependent ROS generation that was responsible for MLC phosphorylation. Our current findings demonstrating that MLC phosphorylation is associated with TJ disruption are in agreement with studies examining the role of monocyte adhesion to and diapedesis across the BBB (16, 25, 34). Afonso *et al.* (25) observed an MLC phosphorylation-dependent BBB disruption when HBECs were cocultured with retrovirus-infected lymphocytes. In addition, monocytes have been demonstrated to traverse the BBB by a matrix metalloproteinase-dependent degradation of occludin (34). Interestingly, monocytes isolated from EAE animals at the peak of the disease cross the BBB by directly inducing oxidative stress in BECs (16), which is paralleled by cytoskeleton rearrangements and the redistribution and disappearance of the TJ molecule occludin (36). Therefore, we studied the question whether IL-17A treatment affects monocyte adhesion and transendothelial migration in our BBB model. We observed increased adhesion of the monocytotic cell line JAWSII to bEnd.3 cells treated with IL-17A, and this effect was accompanied by increased expression of the adhesion molecule ICAM-1. This finding is in contrast to the data of Kebir *et al.* (5), who did not observe an increase in ICAM-1 expression after IL-17A treatment. This discrepancy may be explained by species differences between human and murine BECs. Nevertheless, ICAM-1 together with other cell adhesion molecules (*e.g.*, activated lymphocyte cell adhesion molecule) plays an important role in leukocyte recruitment in MS and EAE (33, 38). After the adhesion to inflamed BECs expressing ICAM-1, monocytes transmigrate across the BBB by a chemoattractant-mediated mechanism, as was also suggested for IL-17A by Kebir *et al.* (5). Because cytokine-induced activation of endothelial NAD(P)H oxidase is associated with an increased release of monocyte chemoattractant protein-1 (39), we hypothesize that a similar mechanism is responsible for the transmigration of the monocyte cell line JAWSII across our murine BBB.

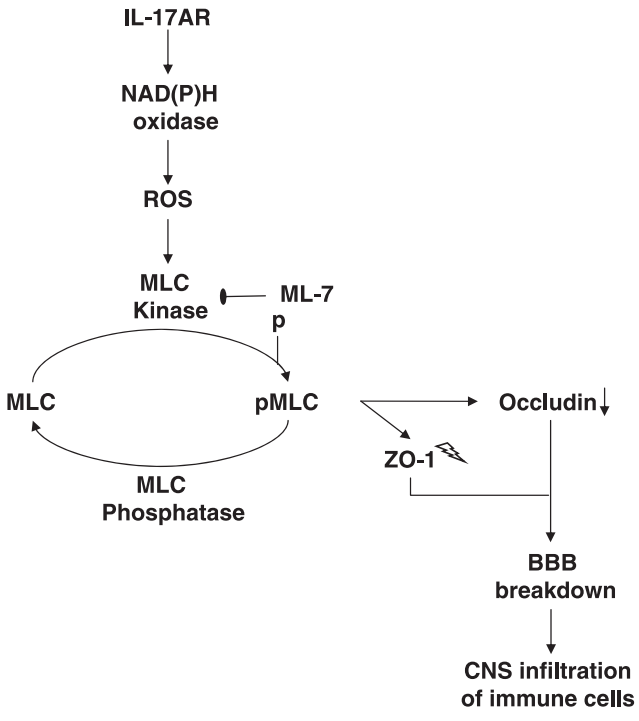

Figure 6. Model of IL-17A-induced BBB disruption.

We were able to translate our results obtained in tissue culture to an *in vivo* model. We hypothesize that IL-17A or possibly also other inflammatory cytokines produced by Th1 and Th17 cells caused effects at the BBB *in vivo*, similar to what we observed in the cell culture model. This hypothesis is supported by the fact that treatment with ML-7 results in less infiltration of inflammatory cells and therefore reduced clinical signs of the disease. In good agreement with the *in vitro* data, ML-7 treatment resulted in reduced BBB disruption, as demonstrated by reduced EB and IgG extravasation as well as endothelial pMLC down-regulation. These findings are further strengthened by the observations of Kebir *et al.* (5), who reported reduced occludin expression in the spinal cords of EAE animals. Various studies demonstrated the involvement of ROS in EAE and MS mainly by showing the protective effects of antioxidants or the up-regulation of antioxidants in lesions (16–18). However, a direct analysis of ROS formation in EAE is lacking. To get a deeper insight into CNS ROS formation in EAE we analyzed oxidative stress by *in situ* DHE stainings. In line with the indirect findings of others, we could demonstrate for the first time that ROS formation is enhanced in spinal cord endothelial cells, as well as in the complete spinal cord homogenate of EAE animals.

To further strengthen the *in vitro* data, EAE experiments were conducted in IL-17A$^{-/-}$ mice. IL-17A$^{-/-}$ mice showed lower levels of oxidative stress in spinal cord homogenates, less BBB disruption (demonstrated by decreased IgG extravasation), and reduced MLC phosphorylation. We and others have shown that IL-17A-deficient mice are less susceptible to EAE, although we could also show that disease also progresses without IL-17A, IL-17F, or both cytokines (22, 40, 41). Our current findings demonstrate that IL-17A contributes to the permeabilization of the BBB and in the absence of IL-17A, disease is reduced but not eliminated. IL-17A therefore has a nonredundant role in

CNS disease progression that contributes to the eventual disease severity but is not essential for disease development altogether. Nevertheless, our findings provide a new mechanism to antagonize the effect of proinflammatory cytokines and, in particular, that of IL-17A on the integrity of the BBB and therefore suggest a novel therapeutic strategy that could be used in the future to prevent or reduce the effects of CNS inflammatory diseases such as MS. FJ

This work was supported by the Interdisziplinärer Forschungsschwerpunkt Neurowissenschaften at the University of Mainz (C.R.W.K., H.L., and A.W.), by the Hertie Foundation (C.R.W.K. and A.W.), by Deutsche Forschungsgemeinschaft grant SFB TR52/C2 (A.W.), and by funds from the Boehringer Ingelheim Stiftung (A.W.). Parts of this work represent partial fulfillment of the requirements for the Ph.D. thesis of J.H.

REFERENCES

1. Frohman, E. M., Racke, M. K., and Raine, C. S. (2006) Multiple sclerosis—the plaque and its pathogenesis. *N. Engl. J. Med.* **354,** 942–955
2. Floris, S., Blezer, E. L. A., Schreibelt, G., Döpp, E., van der Pol, S. M. A., Schadee-Eestermans, I. L., Nicolay, K., Dijkstra, C. D., and de Vries, H. E. (2004) Blood-brain barrier permeability and monocyte infiltration in experimental allergic encephalomyelitis: a quantitative MRI study. *Brain* **127,** 616–627
3. Prat, A., Biernacki, K., Lavoie, J., Poirier, J., Duquette, P., and Antel, J. P. (2002) Migration of multiple sclerosis lymphocytes through brain endothelium. *Arch. Neurol.* **59,** 391–397.55
4. Wong, D., Prameya, R., and Dorovini-Zis, K. (2007) Adhesion and migration of polymorphonuclear leukocytes across human brain microvessel endothelial cells are differentially regulated by endothelial cell adhesion molecules and modulate monolayer permeability. *J. Neuroimmunol.* **184,** 136–148
5. Kebir, H., Kreymborg, K., Ifergan, I., Dodelet-Devillers, A., Cayrol, R., Bernard, M., Giuliani, F., Arbour, N., Becher, B., and Prat, A. (2007) Human TH17 lymphocytes promote blood-brain barrier disruption and central nervous system inflammation. *Nat. Med.* **13,** 1173–1175
6. Rouvier, E., Luciani, M. F., Mattéi, M. G., Denizot, F., and Golstein, P. (1993) CTLA-8, cloned from an activated T cell, bearing AU-rich messenger RNA instability sequences, and homologous to a herpesvirus saimiri gene. *J. Immunol.* **150,** 5445–5456
7. Matusevicius, D., Kivisäkk, P., He, B., Kostulas, N., Ozenci, V., Fredrikson, S., and Link, H. (1999) Interleukin-17 mRNA expression in blood and CSF mononuclear cells is augmented in multiple sclerosis. *Mult. Scler.* **5,** 101–104
8. Lubberts, E., Joosten, L. A., Oppers, B., van den Bersselaar, L., Coenen-de Roo, C. J., Kolls, J. K., Schwarzenberger, P., van de Loo, F. A., and van den Berg, W. B. (2001) IL-1-independent role of IL-17 in synovial inflammation and joint destruction during collagen-induced arthritis. *J. Immunol.* **167,** 1004–1013
9. Yen, D., Cheung, J., Scheerens, H., Poulet, F., McClanahan, T., McKenzie, B., Kleinschek, M. A., Owyang, A., Mattson, J., Blumenschein, W., Murphy, E., Sathe, M., Cua, D. J., Kastelein, R. A., and Rennick, D. (2006) IL-23 is essential for T cell-mediated colitis and promotes inflammation via IL-17 and IL-6. *J. Clin. Invest.* **116,** 1310–1316
10. Wong, C. K., Ho, C. Y., Li, E. K., and Lam, C. W. (2000) Elevation of proinflammatory cytokine (IL-18, IL-17, IL-12) and Th2 cytokine (IL-4) concentrations in patients with systemic lupus erythematosus. *Lupus* **9,** 589–593
11. Röhn, T. A., Jennings, G. T., Hernandez, M., Grest, P., Beck, M., Zou, Y., Kopf, M., and Bachmann, M. F. (2006) Vaccination against IL-17 suppresses autoimmune arthritis and encephalomyelitis. *Eur. J. Immunol.* **36,** 2857–2867
12. Uyttenhove, C., and van Snick, J. (2006) Development of an anti-IL-17A auto-vaccine that prevents experimental auto-immune encephalomyelitis. *Eur. J. Immunol.* **36,** 2868–2874
13. Koch, M., Ramsaransing, G. S. M., Arutjunyan, A. V., Stepanov, M., Teelken, A., Heersema, D. J., and de Keyser, J. (2006) Oxidative stress in serum and peripheral blood leukocytes in patients with different disease courses of multiple sclerosis. *J. Neurol.* **253,** 483–487
14. Kuhlmann, C. R. W., Tamaki, R., Gamerdinger, M., Lessmann, V., Behl, C., Kempski, O. S., and Luhmann, H. J. (2007) Inhibition of the myosin light chain kinase prevents hypoxia-induced blood-brain barrier disruption. *J. Neurochem.* **102,** 501–507
15. Lagrange, P., Romero, I. A., Minn, A., and Revest, P. A. (1999) Transendothelial permeability changes induced by free radicals in an in vitro model of the blood-brain barrier. *Free Radic. Biol. Med.* **27,** 667–672
16. Schreibelt, G., Musters, R. J. P., Reijerkerk, A., de Groot, L. R., van der Pol, S. M. A., Hendrikx, E. M. L., Döpp, E. D., Dijkstra, C. D., Drukarch, B., and de Vries, H. E. (2006) Lipoic acid affects cellular migration into the central nervous system and stabilizes blood-brain barrier integrity. *J. Immunol.* **177,** 2630–2637
17. Schreibelt, G., van Horssen, J., Haseloff, R. F., Reijerkerk, A., van der Pol, S. M. A., Nieuwenhuizen, O., Krause, E., Blasig, I. E., Dijkstra, C. D., Ronken, E., and de Vries, H. E. (2008) Protective effects of peroxiredoxin-1 at the injured blood-brain barrier. *Free Radic. Biol. Med.* **45,** 256–264
18. Van Horssen, J., Schreibelt, G., Drexhage, J., Hazes, T., Dijkstra, C. D., van der Valk, P., and de Vries, H. E. (2008) Severe oxidative damage in multiple sclerosis lesions coincides with enhanced antioxidant enzyme expression. *Free Radic. Biol. Med.* **45,** 1729–1737
19. Brown, R. C., Morris, A. P., and O'Neil, R. G. (2007) Tight junction protein expression and barrier properties of immortalized mouse brain microvessel endothelial cells. *Brain Res.* **1130,** 17–30
20. Benton, R. L., Maddie, M. A., Worth, C. A., Mahoney, E. T., Hagg, T., and Whittemore, S. R. (2008) Transcriptomic screening of microvascular endothelial cells implicates novel molecular regulators of vascular dysfunction after spinal cord injury. *J. Cereb. Blood Flow Metab.* **28,** 1771–1785
21. Kuhlmann, C. R., Librizzi, L., Closhen, D., Pflanzner, T., Lessmann, V., Pietrzik, C. U., de Curtis, M., and Luhmann, H. J. (2009) Mechanisms of C-reactive protein-induced blood-brain barrier disruption. *Stroke* **40,** 1458–1466
22. Haak, S., Croxford, A. L., Kreymborg, K., Heppner, F. L., Pouly, S., Becher, B., and Waisman, A. (2009) IL-17A and IL-17F do not contribute vitally to autoimmune neuro-inflammation in mice. *J. Clin. Invest.* **119,** 61–69
23. Minagar, A., and Alexander, J. S. (2003) Blood-brain barrier disruption in multiple sclerosis. *Mult. Scler.* **9,** 540–549
24. Tzartos, J. S., Friese, M. A., Craner, M. J., Palace, J., Newcombe, J., Esiri, M. M., and Fugger, L. (2008) Interleukin-17 production in central nervous system-infiltrating T cells and glial cells is associated with active disease in multiple sclerosis. *Am. J. Pathol.* **172,** 146–155
25. Afonso, P. V., Ozden, S., Prevost, M., Schmitt, C., Seilhean, D., Weksler, B., Couraud, P., Gessain, A., Romero, I. A., and Ceccaldi, P. (2007) Human blood-brain barrier disruption by retroviral-infected lymphocytes: role of myosin light chain kinase in endothelial tight-junction disorganization. *J. Immunol.* **179,** 2576–2583
26. Haorah, J., Schall, K., Ramirez, S. H., and Persidsky, Y. (2008) Activation of protein tyrosine kinases and matrix metalloproteinases causes blood-brain barrier injury: novel mechanism for neurodegeneration associated with alcohol abuse. *Glia* **56,** 78–88
27. Lander, H. M. (1997) An essential role for free radicals and derived species in signal transduction. *FASEB J.* **11,** 118–124
28. Garcia, J. G., Liu, F., Verin, A. D., Birukova, A., Dechert, M. A., Gerthoffer, W. T., Bamberg, J. R., and English, D. (2001) Sphingosine 1-phosphate promotes endothelial cell barrier integrity by Edg-dependent cytoskeletal rearrangement. *J. Clin. Invest.* **108,** 689–701

29. Dudek, S. M., Jacobson, J. R., Chiang, E. T., Birukov, K. G., Wang, P., Zhan, X., and Garcia, J. G. N. (2004) Pulmonary endothelial cell barrier enhancement by sphingosine 1-phosphate: roles for cortactin and myosin light chain kinase. *J. Biol. Chem.* **279,** 24692–24700
30. Verin, A. D., Csortos, C., Durbin, S. D., Aydanyan, A., Wang, P., Patterson, C. E., and Garcia, J. G. (2000) Characterization of the protein phosphatase 1 catalytic subunit in endothelium: involvement in contractile responses. *J. Cell. Biochem.* **79,** 113–125
31. Noseworthy, J. H., Lucchinetti, C., Rodriguez, M., and Weinshenker, B. G. (2000) Multiple sclerosis. *N. Engl. J. Med.* **343,** 938–952
32. Lucchinetti, C., Brück, W., Parisi, J., Scheithauer, B., Rodriguez, M., and Lassmann, H. (2000) Heterogeneity of multiple sclerosis lesions: implications for the pathogenesis of demyelination. *Ann. Neurol.* **47,** 707–717
33. Cayrol, R., Wosik, K., Berard, J. L., Dodelet-Devillers, A., Ifergan, I., Kebir, H., Haqqani, A. S., Kreymborg, K., Krug, S., Moumdjian, R., Bouthillier, A., Becher, B., Arbour, N., David, S., Stanimirovic, D., and Prat, A. (2008) Activated leukocyte cell adhesion molecule promotes leukocyte trafficking into the central nervous system. *Nat. Immunol.* **9,** 137–145
34. Reijerkerk, A., Kooij, G., van der Pol, S. M. A., Khazen, S., Dijkstra, C. D., and de Vries, H. E. (2006) Diapedesis of monocytes is associated with MMP-mediated occludin disappearance in brain endothelial cells. *FASEB J.* **20,** 2550–2552
35. Bettelli, E., Oukka, M., and Kuchroo, V. K. (2007) T_H-17 cells in the circle of immunity and autoimmunity. *Nat. Immunol.* **8,** 345–350
36. Schreibelt, G., Kooij, G., Reijerkerk, A., van Doorn, R., Gringhuis, S. I., van der Pol, S., Weksler, B. B., Romero, I. A., Couraud, P., Piontek, J., Blasig, I. E., Dijkstra, C. D., Ronken, E., and de Vries, H. E. (2007) Reactive oxygen species alter brain endothelial tight junction dynamics via RhoA, PI3 kinase, and PKB signaling. *FASEB J.* **21,** 3666–3676
37. Haorah, J., Heilman, D., Knipe, B., Chrastil, J., Leibhart, J., Ghorpade, A., Miller, D. W., and Persidsky, Y. (2005) Ethanol-induced activation of myosin light chain kinase leads to dysfunction of tight junctions and blood-brain barrier compromise. *Alcohol Clin. Exp. Res.* **29,** 999–1009
38. Steffen, B. J., Butcher, E. C., and Engelhardt, B. (1994) Evidence for involvement of ICAM-1 and VCAM-1 in lymphocyte interaction with endothelium in experimental autoimmune encephalomyelitis in the central nervous system in the SJL/J mouse. *Am. J. Pathol.* **145,** 189–201
39. Volk, T., Hensel, M., Schuster, H., and Kox, W. J. (2000) Secretion of MCP-1 and IL-6 by cytokine stimulated production of reactive oxygen species in endothelial cells. *Mol. Cell. Biochem.* **206,** 105–112
40. Komiyama, Y., Nakae, S., Matsuki, T., Nambu, A., Ishigame, H., Kakuta, S., Sudo, K., and Iwakura, Y. (2006) IL-17 plays an important role in the development of experimental autoimmune encephalomyelitis. *J. Immunol.* **177,** 566–573
41. Hofstetter, H. H., Ibrahim, S. M., Koczan, D., Kruse, N., Weishaupt, A., Toyka, K. V., and Gold, R. (2005) Therapeutic efficacy of IL-17 neutralization in murine experimental autoimmune encephalomyelitis. *Cell. Immunol.* **237,** 123–130

Received for publication July 20, 2009.
Accepted for publication October 29, 2009.